Expanded View Figures

Figure EV1. L1 RNP cytosolic aggregates are not sensitive to treatment with 3% 1,6 Hexanediol.

A Maximum intensity projections across Z stacks of example images from indicated mESCs immunostained for L1 ORF1p (red) and MOV10 (green) with nuclei stained with DAPI (blue). Gray box mark position of the insets (n = 3 biological replicates).

B Maximum intensity projections across Z stacks of example images from indicated mESCs immunostained for LC3B (red) and MOV10 (green) with nuclei stained with DAPI (blue). The gray square depicts position of inset (n = 3 technical replicates).

Data information: Scale bar 5 μm.

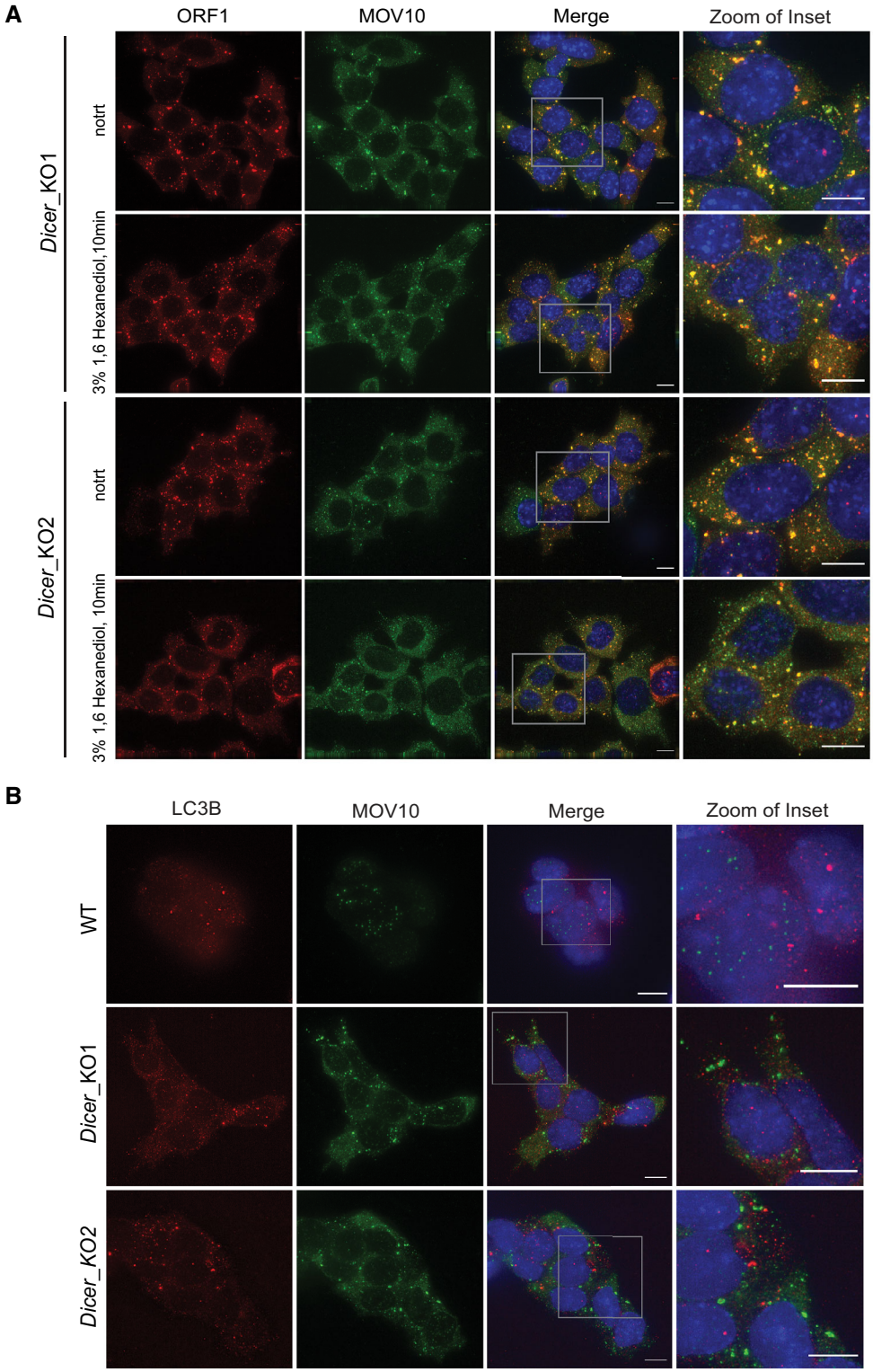

Figure EV1.

Figure EV2. Generation of mESCs upregulating L1 expression using CRISPRa.

A Schematic depicting full-length L1 element and summary of CRISPRa. To generate $L1^{UP}$ cells, mESCs were co-transfected with plasmid encoding catalytically dead Cas9 protein (dCas9) fused to VP160 and sgRNAs that (1) targeted the fusion protein to the 5'UTR sequence of Tf L1 family allowing (2) recruitment of transcription factors and (3) transcription machinery to (4) upregulate L1 transcription.

B Sequence alignment of 5'UTR sequences of murine L1 Tf, Gf and A subfamilies. The two sgRNA sequences used to upregulate L1 expression are indicated in blue and green, with protospacer adjacent motifs (PAM) in bold.

C RT–qPCR analysis to quantitate *Dicer*, and L1 RNA expression levels in the depicted cell lines. *Rrm2* was utilized for normalization, and graphs depict fold change in transcript levels compared to WT which was set to one ($n = 3$ technical replicates).

D Representative northern blot analysis probed for L1 RNA to assess L1 transcript length and expression levels in the engineered $L1^{UP}$ Cl1, Cl2 as compared with Ctrl cells. Arrow points to full-length L1 transcript. Ethidium bromide staining of 28S RNA was used to confirm equal loading ($n = 3$ technical replicates).

E Differential gene expression from RNA-seq analysis of *Dicer*_KO vs. WT mESCs plotted using previously published data (Bodak *et al*, 2017).

F RT–qPCR analysis to confirm upregulation of *Mov10* in *Dicer*_KO cells. *Rrm2* was utilized for normalization, and graphs depict fold change in transcript levels in the indicated cell lines as compared to WT which was set to one ($n = 3$ technical replicates).

Data information: In (C and F) bar graphs are mean ± SD. *P*-value computed using unpaired *t*-test comparing results from individual cells to WT mESCs. ***P-value < 0.0005, **P-value < 0.001, *P-value < 0.05. In (E) each dot represents a single gene. Position for *Mov10* in the graph is marked. Values for Log2 fold change (Log2FC) were plotted on the x-axis and Log10 of the P-value on the y-axis.
Source data are available online for this figure.

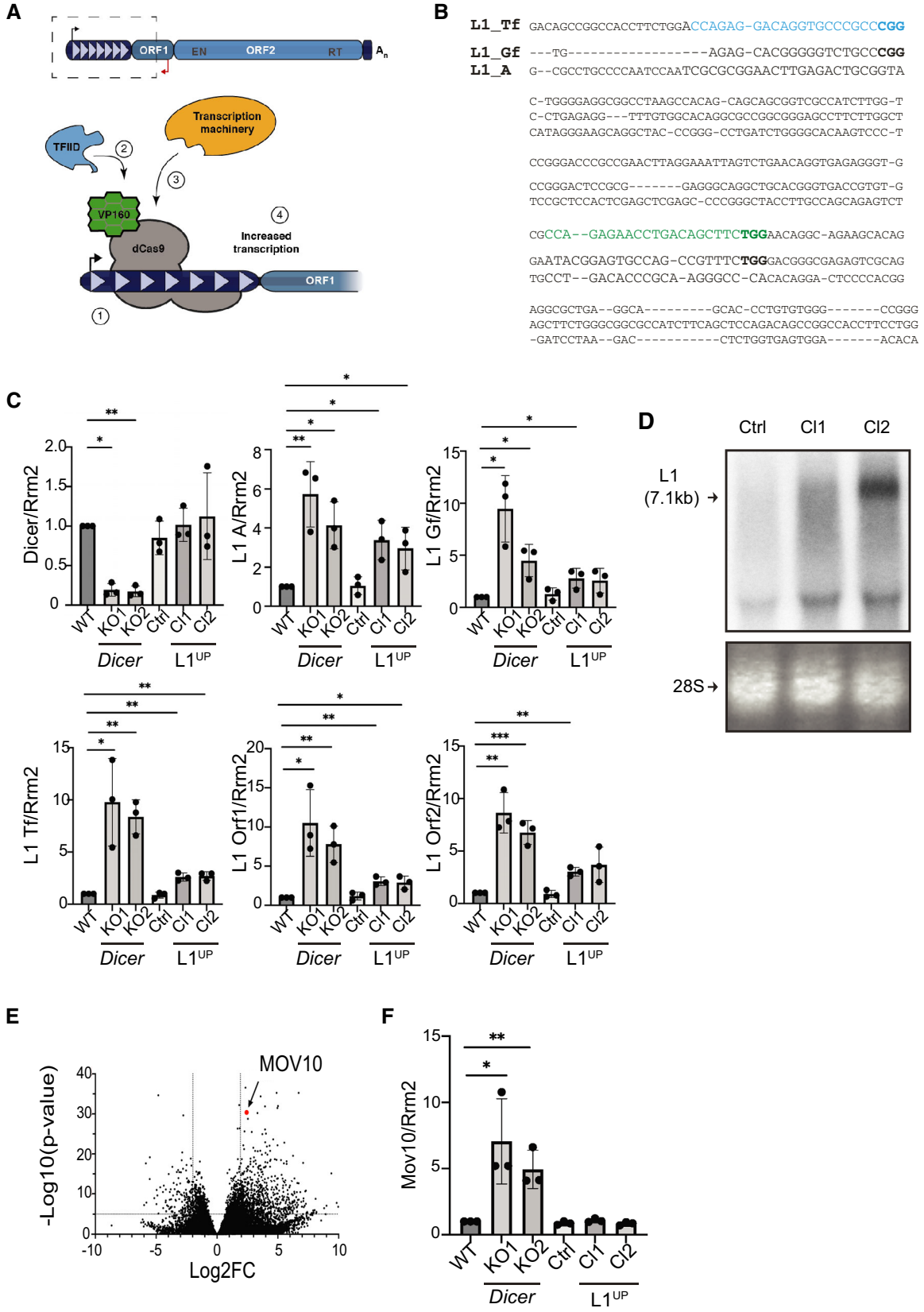

Figure EV2.

Figure EV3. Posttranscriptional regulation of *Mov10* by miRNAs in mESCs.

A Log2 normalized count of miRNAs in WT mESCs from previously published small RNA-seq data (Ngondo *et al*, 2018; Müller *et al*, 2022). miRNAs predicted to target 3'UTR of MOV10 are in red.

B Schematic of 3'UTR sequence of *Mov10* RNA helicase. Location and sequence of WT and mutant (MUT) miRNA response elements (MREs) for mouse miR-138-5p (red), miR-30-5p (blue) miR-16-5p (blue) and miR-153-3p (orange) predicted to target *Mov10* (ENSMUST00000168015.8) are color coded based on seed type matching for respective miRNAs.

C Western Blot analysis to assess the expression of L1 ORF1p, MOV10, AGO2 in the indicated cell lines, immunoblot with TUBULIN served to control for loading. KO status was confirmed by probing for DROSHA and DICER ($n = 3$ technical replicates). Asterisk marks nonspecific band.

D Schematic depicting design of experiment for processing samples along with representative gels for WB analysis and quantitation of MOV10 and TUBULIN signals in *Drosha*_KO cells transfected with ctrl or mimic miRNA either singly or in pairs ($n = 3$–6 biological replicates). Untreated WT cells are shown for comparison of MOV10 expression.

Data information: Bar graphs are mean intensity ± SD of MOV10 normalized by TUBULIN. Values are relative to transfection for the Ctrl mimic that was set to 1. *P*-values were computed using ordinary one-way ANOVA test ****P-value < 0.0001 and *P-value < 0.05.
Source data are available online for this figure.

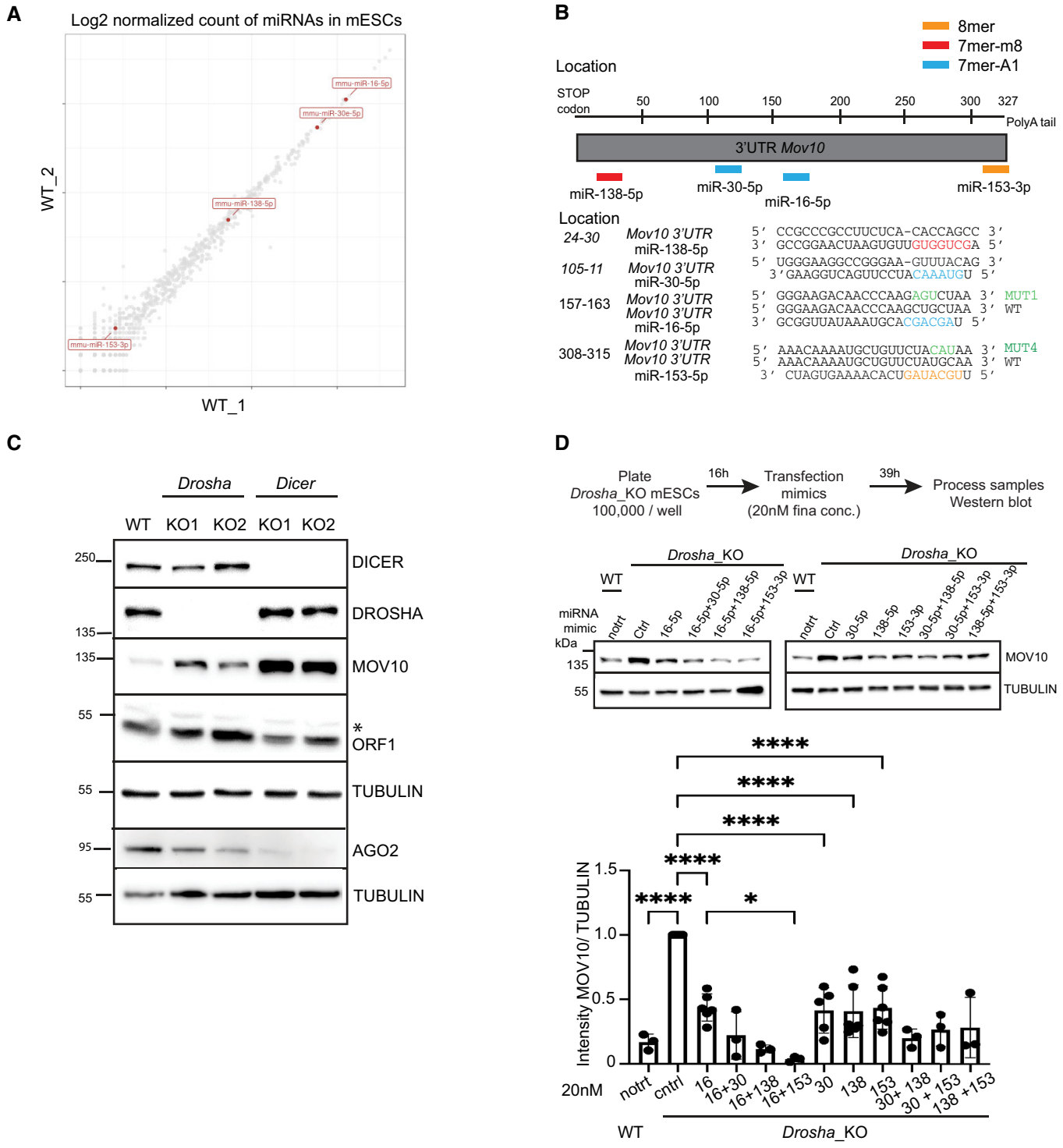

Figure EV3.

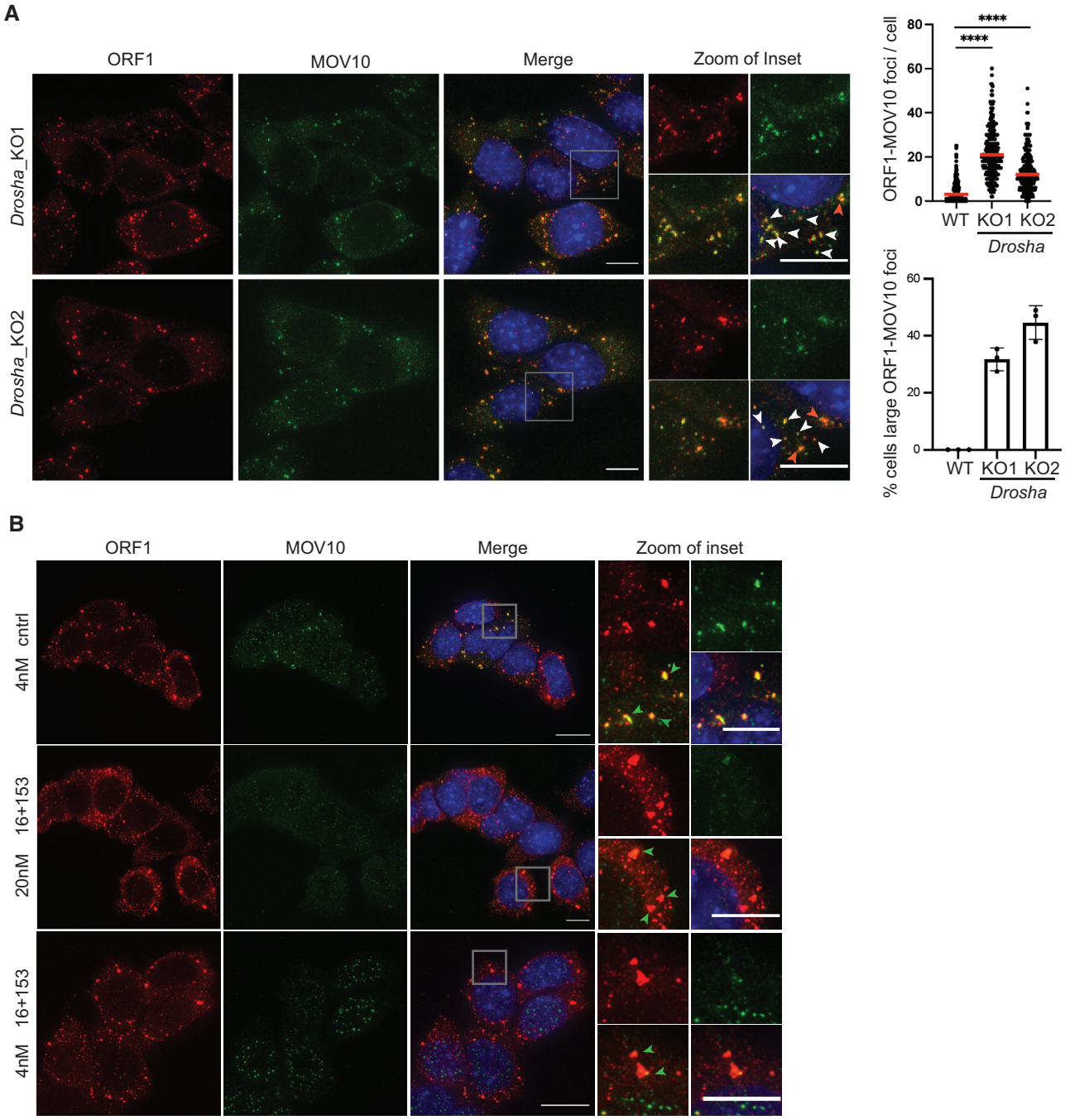

Figure EV4. Cytosolic L1 RNP foci in *Drosha*_KO cells.

A Maximum intensity projections across Z stacks of example images from indicated *Drosha*_KO mESCs immunostained for L1 ORF1p (red) combined with MOV10 (green) and nuclei stained with DAPI (blue). The gray square marks position of the inset. White arrow heads point to cytoplasmic foci where ORF1p and MOV10 co-localize. Scatter plot shows the number of co-localized L1 Tf-ORF1 foci in the cytoplasm per cell (288 *Drosha*_KO1, 299 *Drosha*_KO2 cells, 293 WT (same as Fig 1)). Red arrow heads point to relatively larger sized L1 RNP foci. Bar graphs are mean values of percentage of cells with large ORF1-MOV10 foci co-localizing in the cytoplasm ($n = 3$ technical replicates).

B Maximum intensity projections across Z stacks of example images from *Drosha*_KO2 cells transfected with either control or indicated concentration of miR-16-5p and miR-153-3p miRNA mimics ($n = 3$). The gray square marks position of the inset. Green arrow heads point to relatively large cytoplasmic foci where ORF1p and MOV10 co-localize.

Data information: In (A) data are depicted as scatter plots where circles are single data points representing number of co-localized ORF1p-MOV10 foci in the cytoplasm per cell, red bar is median. Statistical analysis was performed using Mann–Whitney *U* test and ****P-value < 0.0001. Bar graphs represent mean ± SD. Scale bar 5 μm. Source data are available online for this figure.